Towards predictive modelling for concrete

I. Cullis, M. Hinton, S. Gilbert, P. Church, D. Porter, T. Andrews, W. Proud, A. Pullen

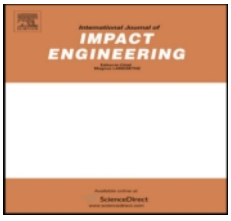

Title: Towards predictive modelling for concrete

Authors: I. Cullis, M. Hinton, S. Gilbert, P. Church, D. Porter, T. Andrews, W. Proud, A. Pullen

PII: S0734-743X(08)00191-7
DOI: 10.1016/j.ijimpeng.2008.07.050
Reference: IE 1673

To appear in: *International Journal of Impact Engineering*

Received Date:
Revised Date:
Accepted Date:

Please cite this article as: Cullis I, Hinton M, Gilbert S, Church P, Porter D, Andrews T, Proud W, Pullen A. Towards predictive modelling for concrete, International Journal of Impact Engineering (2008), doi: 10.1016/j.ijimpeng.2008.07.050

Towards predictive modelling for concrete

I. Cullis[*1], M. Hinton[1], S. Gilbert[1], P. Church[1], D. Porter[2], T. Andrews[2]
W. Proud[3], A. Pullen[4]

[1]*QinetiQ, Fort Halstead, Kent, United Kingdom*
[2]*QinetiQ, Farnborough, Hampshire, United Kingdom*
[3]*Cavendish Laboratory, Cambridge University, United Kingdom*
[4]*Imperial College, London, United Kingdom*

Abstract

Simulations are becoming an increasingly important part of the weapon design cycle allowing the investigation of more parameters in warhead concepts. This relies on a thorough verification & validation process for the simulation tools, which enables a cost effective approach to down-selecting concepts for full-scale experiments. A key factor in this process applied to the design of warheads to defeat hard (structural) targets is the development of truly physically based material models for geological materials where constants are either derived or measured. The paper describes this general approach and highlights aspects of its initial application to kinetic energy (KE) penetration and suggests areas for future investigation.

Keywords: Material Models, Concrete, Penetration, Experiments, Numerical Simulation

1. Introduction

The defeat of a wide range of structural targets is becoming an increasingly important requirement, since these targets usually comprise significant aspects of the infrastructure of the opposing forces. Simulations integrated with precise experiments are becoming an increasingly important part of the design cycle for a new weapon system capable of defeating an ever more diverse target set.

From a design viewpoint, the first challenge is to characterise the wide spectrum of building materials (geological and man-made) in an accurate, rapid and cost effective manner such that both the local, high strain rate, impact response and the longer time, global, structural response can be simulated.

Within QinetiQ an experimental test methodology is now in place to derive the necessary information to encompass the Quasi-Static (QS) and high strain rate loading regimes. The methodology takes account of the intrinsic differences in the behaviour of geological materials from the more widely

[*]Corresponding author. Tel.: +44 1959 514889; fax: +44 1959 516050.
E-mail address: igcullis@qinetiq.com

understood response of metals. In metals the general deformation behaviour, based on dislocation mechanics can be separated from the ductile fracture process, based on void growth. However, geological materials deform and fracture through a micro-cracking process simultaneously and thus deformation and fracture cannot be separated.

This paper describes the general methodology used to construct these geological material models through an integration of experiments and simulation tools. The use of the methodology is exemplified using the penetration mechanisms of a hypervelocity penetrator impacting spaced reinforced concrete panels.

2. General Approach

The general approach adopted is to integrate precise experiments with simulations that utilise state of the art theoretical developments in materials science.

The overall objective is to provide a truly predictive capability, defined here as agreement to within 5% of experimental results or experimental error, whichever is the larger. The approach being taken by QinetiQ to attain this highly ambitious goal is to provide the highest accuracy within the hydrocode numerical schemes, the material models and the material characterisation experiments, coupled with the implementation of a comprehensive verification & validation process. Considerable efforts have been directed to improve the accuracy of the in-house Eulerian hydrocode 'GRIM' and the QinetiQ customised version of the LLNL Lagrangian hydrocode DYNA. The goal of providing a predictive modelling capability for problems that involve isotropic metals has largely been achieved [1] with the development of physically based constitutive and fracture models, where all constants were either measured or derived.

Geological materials pose a far sterner challenge from a modelling perspective - in the regimes of interest, determining the shock equation of state (EOS) is intimately linked to the constitutive and fracture behaviour. The goal in this area is to develop simple physically-based material models. In addition it is important that these constants have physical meaning as opposed to being fitting parameters.

2.1 Equation Of State Development

A totally different approach, based on Quantitative Structure/Property Modelling (QSPM), has therefore been applied to establish the shock EOS directly from material properties, for example density, such that all constants are measured or derived. The approach has been applied to geological materials [2] and is based on an implicit assumption that many geological materials are a derivative of different crystal forms of silica (i.e. Crystobalite, Coesite, α-quartz, Stishovite).

The technique is based on a method used to predict the structural properties of polymers - Group Interaction Modelling (GIM) [3]. The technique uses quantum mechanics to predict the relationship between energy and separation distance between adjacent (but not chemically bonded) groups of atoms in a molecular structure. This space between groups of atoms can also naturally include the porosity in geological materials, i.e. the technique can work at both the atomic and microstructural length scales. A Lennard-Jones function, standard for intermolecular interactions, describes these interactions very well for most chain molecules based upon carbon or silicon lattices and embodies all the fundamental contributions to bond energy. To a first approximation, GIM assumes that chemical bonds do not

deform significantly, relative to the weak electronic interactions between the groups. The general form of a potential energy well for intermolecular interactions is shown in Fig. 1.

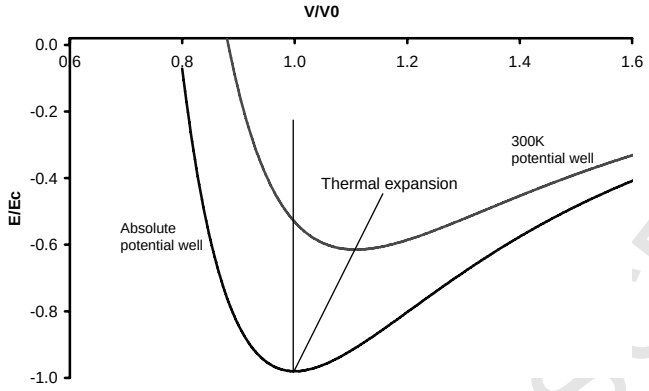

Fig. 1. A potential well for intermolecular energy

Energy, E, is expressed relative to the depth of the potential energy well, E_c, and dimensions are given as volume, V, relative to the volume at the absolute depth of the potential energy well, V_0 (the molar volume adjusted for thermal expansion). Note that energies for bonding are negative. As positive energy (such as thermal energy, H_T) is increased, the interaction dimensions move away from the minimum energy position to two possible values on either side of the minimum. Generally, the potential well is asymmetric, such that the equilibrium mean position of the new well minimum moves to higher volumes to cause thermal expansion in the material. The pressure-volume relationship is valid for any dry silica polymorph and has as its parameters only V_0 and the molar volume at zero pressure and temperature, T, V_T.

$$P = 0.34\left(\left(\frac{V_0}{V}\right)^3 - \left(\frac{V_0}{V}\right)^5 - \left(\frac{V_0}{V_T}\right)^3 + \left(\frac{V_0}{V_T}\right)^5\right) \tag{1}$$

Results (in Pressure/Volume space) for the prediction of the shock EOS for different forms of silica are compared with experimental data in Fig. 2 – giving a high confidence level that the approach is valid for these materials. This is demonstrated by applying the technique to real geological materials and predicting their shock Hugoniot behaviour. This is shown in Fig. 3 for sand, granite, and various concretes.

These results are significant since they demonstrate that the QSPM approach can handle composite materials, such as concrete, as well as highly porous materials. As an example the predicted result for sand (shown in Fig. 3) takes into account the porosity of 42%; the approach can also predict the effect of water saturation. The only parameter required, assuming that the material constituents and their volume fractions are known, is the material density. The equation of state has also been extended to include phase changes under high compressive stress, where the silica changes from quartz to the higher density crystal form of Stishovite.

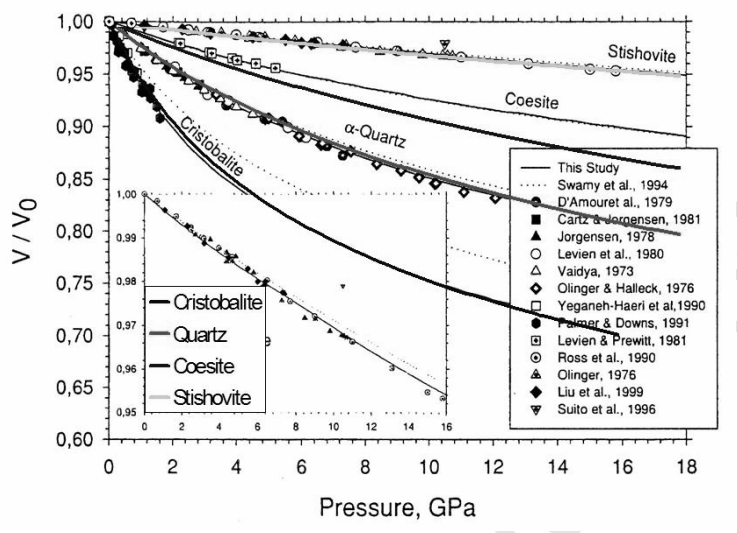

Fig. 2. Comparison of Porter-Gould EOS for PV data for silica

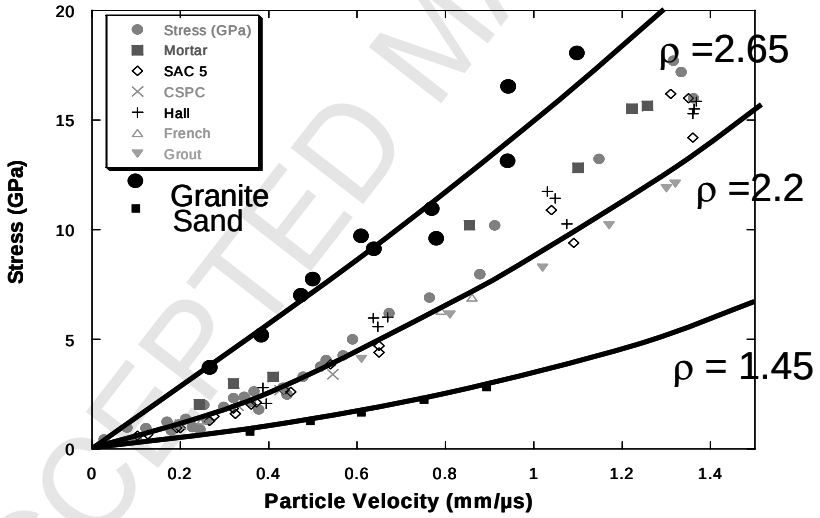

Fig. 3. Comparison of Porter-Gould EOS with Hugoniot data

2.2 Validation Experiments

A key aspect of material model development is the assessment of its validity over a wide range of loading regimes and stress states. This demands precise experiments in sufficient quantity to be statistically significant and that measure the relevant properties. In terms of geological materials the key

characterisation tests are: triaxial cell tests; Hopkinson bar in compression and tension; and, plate impact.

These tests are supplemented by a variety of additional impact and penetration experiments, depending on the lethal mechanism being considered. Triaxial tests are performed, usually under quasi-static loading conditions such that the flow stress as a function of pressure is measured. The specimen is generally confined either passively or actively under hydrostatic pressure [4], with strain gauges measuring axial and radial strains, to derive the overall stress-state. Within the UK, Imperial College and Sheffield University have played the principal role in the generation of a substantial database on sands, concretes and a wide variety of geological materials.

To understand the behaviour of material at high strain rates (i.e. $>10^3 s^{-1}$) compression and tensile tests are performed on a Hopkinson bar. These measure the dynamic stress v strain of the specimen, which for compression is usually, but not always confined. In tension the main output is a measure of the tensile strength as a function of strain rate [5].

Plate impact tests are used to measure the shock Hugoniot EOS for the material under uniaxial strain. In these tests a flyer plate impacts a target under uniaxial strain conditions over a range of velocities. Manganin stress gauges and VISAR are used to measure the stress and particle velocity within the sample, which is used to derive the shock Hugoniot. Within the UK there is now a wealth of shock data on a range of concretes, sands and rocks.

3. Demonstration Of Approach

The approach outlined above is demonstrated using experimental data of a KE projectile penetrating a series of concrete panels. It should be noted that only the QinetiQ Porter-Gould EOS was used in the simulations as the constitutive model is still being implemented. Our existing constitutive model based on the standard Johnson-Holmquist [6] was therefore used.

3.1 KE penetration

The experimental trials were performed using the Electromagnetic Launch Facility (EMLF) at Kirkcudbright. The target comprised 6 reinforced concrete panels 200mm thick spaced about 2.4m apart and was constructed to be representative of typical building and factory walls, Fig. 4. The target material was well controlled and the compressive strength was measured separately for each panel. The projectile impacted the target normally at $1600 m.s^{-1}$ with close to zero pitch and yaw. Two trials were performed each of which demonstrated that the projectile penetrated 3 panels. The projectile package was constructed from maraging steel with a tungsten alloy core.

The post trial measurements were hole and crater sizes in the target, shown in Table 1, and velocity and shot line estimates of the projectile. The holes in the first panel are relatively consistent and circular, whereas in the subsequent panels the holes are significantly asymmetric. Two obvious interpretations of this are that the projectile is tumbling or that it has fractured and the broken parts are flying off line and contributing to hole formation. The targets also exhibited significant spallation and cracking.

Fig. 4. Representative Target (left), projectile fired out of QinetiQ EM Gun

Table 1. Summary of Experimental Data for Holes In Concrete panels.

	Impact Location (in)		*Hole Size (in)*		*Crater Size (in)*			
	Vert.	*Horz.*	*Entry*	*Exit*	*Entry Depth*	*Entry Diam.*	*Exit Depth*	*Exit Dia.*
Wall 1	95.7	91	1.5	1.5	3.75	10.5	3.25	13.5
Wall 2	96	93	4.25x2.75	3.5x2.5	3	16x16.5	4.5	17x16
Wall 3	97	92	14.5x12	14.25x12	2.75	24.5x25	5.25	25.5x25.5
Wall 4	A=97.5	A=93	N/A	N/A	A=3.75	A=10.5	N/A	N/A
	B=89	B=99	N/A	N/A	B=3.25	B=6.5x7.25	N/A	N/A
Wall 5	N/A	N/A	N/A	N/A	N/A	N/A	N/A	N/A
Wall 6	N/A	N/A	N/A	N/A	N/A	N/A	N/A	N/A

3.2 Simulations

Simulations were performed using QinetiQ GRIM and customised DYNA3D to gain further insight into the penetration mechanisms. For the normal impact case quarter geometry utilised two symmetry planes. For the 1° impact case half symmetry was used, to include the full distance between panels in the simulation to investigate any tumbling of the projectile between panels and also any deviation from the shot line. The simulations were analysed to determine general penetration dynamics, hole and crater sizes and velocity drop between panels.

The hydrocodes embodied the advanced constitutive and fracture models and the simulations were used to explore the mechanisms for break-up of the projectile and target, as well as the sensitivity to slight asymmetries (i.e. pitch/attack angle) on the impact process. The main purpose of the simulations was to identify the mechanisms operating in this regime of high velocity KE penetration. For simplicity it was decided to simulate the normal impact case, where it was known that the projectile impacted the first panel away from the reinforcement bars (i.e. rebar). The material models used for the projectile were the modified Armstrong-Zerilli model [7,8]. The model form is as follows: -

$$\sigma = \left(C_1 + C_5 \varepsilon^n\right)\frac{\mu_T}{\mu_{293}} + C_2 \exp\left[\left(C_3 + C_4 \ln \dot{\varepsilon}\right)T\right] \tag{2}$$

Here C_1 to C_5 and n are constants; σ, ε ,$\dot{\varepsilon}$ and T are respectively stress, strain, strain rate and temperature in K; μ_{293} is the shear modulus at 293K and μ_T is the shear modulus at the current temperature. The constants used for this study, which were derived directly from interrupted tensile tests, were as shown in Table 2.

The Goldthorpe Path Dependent Fracture (PDF) Model was used to describe the multi-mode ductile and shear fracture processes [9]. The form is as follows: -

$$dS = 0.67\, e^{\left[1.5\sigma_n - 0.04\,\sigma_n^{-1.5}\right]} d\varepsilon + A\,\varepsilon_s \qquad (3)$$

where σ_n is the stress triaxiality or (P/Y), dε is the effective plastic strain increment, ε_s is the maximum principle shear strain, A is a constant (from a torsion test), and dS is the damage increment.

Table 2. Constants for modified Armstrong-Zerilli model for maraging steel and tungsten alloy

	Maraging steel	*Tungsten alloy*
C1	1800 MPa	600 MPa
C2	500 MPa	2697 MPa
C3	-0.006	-0.0043
C4	0.00015	0.00017
C5	700 MPa	750 MPa
N	0.5	0.65

Fracture occurs when the damage reaches a critical value Sc, which is determined from examining the neck region in a quasi-static tension test. The damage comprises a tensile component due to void growth and a shear component due to shear localisation. The shear parameter 'A' is determined from a torsion test, which measures the shear strain to failure. Thus the algorithm is a multi-mode failure model, where the tensile failure will dominate for P/Y values <-0.3 and the shear failure will be dominant for the P/Y values -0.3<P/Y<0. In these simulations the damage parameters Sc and 'A' for the tungsten and the maraging steel were estimated from material specification sheets and by comparison with similar materials in the QinetiQ materials database. This yielded values of Sc for the maraging steel and tungsten alloy of 0.2 and an 'A' value for each of 2.0.

The concrete model used was the QinetiQ Porter-Gould EOS combined with a standard Johnson-Holmquist constitutive model for concrete.

3.3 Simulation Results

The simulations demonstrated that the flare of the projectile was broken off during penetration through the throat of the hole in the first panel. The flare strikes the hole in the panel and is then crushed towards the axis subsequently fracturing under the tensile stresses generated. This process is illustrated in figure 5 and demonstrates that tensile failure is the dominant mechanism for the break-up of the flare. This also explains why the hole in the first panel is less than the diameter of the projectile, since the flare is subsequently crushed such that it is predicted to pass through the hole. The other key feature of the penetration process is the significant erosion and failure of the projectile tungsten alloy

nose. In fact the simulations predict that the nose has been completely eroded after penetrating the third panel. This is not surprising since the impact velocity is similar to conventional KE rounds and the strength of concrete in compression can exceed the strength of the nose material and hence induce deformation and erosion.

The simulation of the projectile strike with a 1° pitch angle demonstrated that the path of the projectile is very similar to the normal impact for the first two panels, although the flare does break asymmetrically. Whilst the projectile starts to deviate from its initial flight path in the second panel, the deviation is still relatively small. However, the penetration of the third panel induces significant tumbling (Fig. 5), such that it impacts the fourth panel almost sideways-on, with a significant deviation from the shotline. This is consistent with the projectile only perforating 3 panels in the experiment.

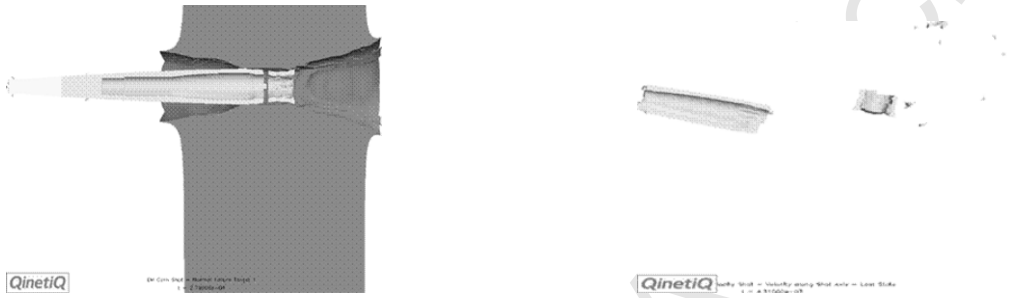

Fig. 5. Projectile fracture in the 1st panel (left) and tumbling on exiting the 3rd panel (right)

The comparison of the simulation results with the experimental hole and crater sizes are shown in Table 3. These show that the simulations predict the hole dimensions in the first panel very well but the subsequent holes are very asymmetric indicating that the projectile is significantly tumbling or breaking up after the first panel. Alternatively the fractured flare may be causing secondary impacts on subsequent panels. It is noted that the simulations do not predict the crater or back surface spall very well and this is primary reason for the need for the improved physically based constitutive model described above.

The GRIM simulations were performed as a direct comparison with DYNA and illustrated the same break-up mechanisms for the projectile as shown in Fig. 6. The predicted hole sizes were similar to those predicted using DYNA.

Table 3. Comparison of predicted and experimental hole sizes

	1st Panel (mm)	2nd Panel (mm)	3rd Panel (mm)
Simulation	41	54	68
Experiment	38	100x38	254x406

A direct comparison of the flare break-up between GRIM and DYNA shows very good correlation, Fig. 6. This implies that the type of numerical scheme is a 2nd order effect and it is the material model that determines whether the simulations are predictive; which has been our experience in general for other applications.

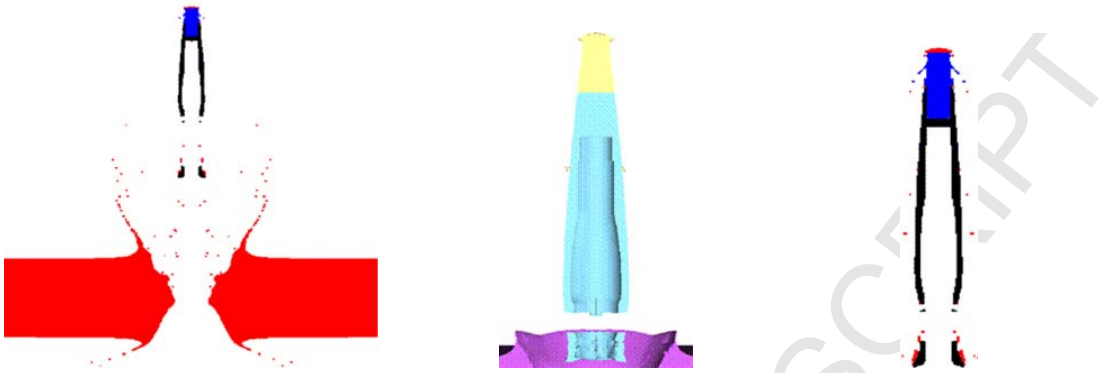

Fig. 6. Projectile after perforation of 1st Panel using GRIM showing fracture of flare (left), Comparison of projectile after perforating first panel between DYNA (centre) and GRIM (right)

4. Constitutive Model Development

The methodology used for the EOS has been extended to the constitutive response including damage evolution. The method will be fully explained in a forthcoming journal publication. The method recognises that concrete is a composite material with a compliant component (sand/cement) and a relatively non-compliant component (aggregate). The model assumes that the elastic and plastic strain is predominantly in the compliant component. The elastic energy density of the fraction of total strain in the cement is taken to be dissipated by collapse of the voids.

The amount of plastic strain with respect to the elastic strain causes the apparent elastic modulus to be reduced. This model is applied to the triaxial cell test and shown to give highly encouraging predictions under constrained uniaxial compression for a model concrete as shown in Fig. 7. The decrease in stress occurs when the specimen is unloaded, i.e. the strain was decreased. The unloading path is different because the apparent elastic modulus has increased. Traditionally this is explained by the void/pore collapse associated with the compressive loading increasing the bulk modulus.

Our interpretation is that the material is stiffer because the ***whole of the composite*** is responding to the unloading rather than just the compliant components. It is important to understand that the EOS does not significantly change the modulus in this test, because the pressures are low.

In ***tension*** the reduction in elastic modulus is due to loss of connectivity between rigid filler particles and binder. An Arrhenius expression in energy is used to estimate the damaged fraction under strain (ε), relative to an activation strain, ε_a, the tensile activation strain for debonding (~0.00015), which affects the Young's modulus (E) via equation 4. In this equation ε is a one dimensional strain and research is currently exploring its interpretation and the resulting implementation of the constitutive model in three dimensions.

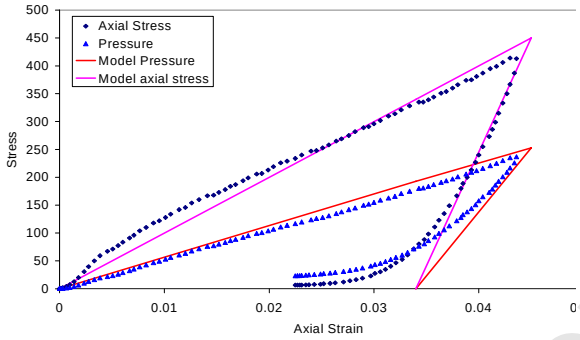

Fig. 7. Comparison of Porter-Gould constitutive model with Quasi-static Triaxial cell data (symbols)

$$E = E_0\left[1 - \exp\left(-\frac{\varepsilon_a^2}{\varepsilon^2}\right)\right] \tag{4}$$

The functional form of the Arrhenius expression for modulus is shown to give a good representation of observed stress-strain relations. The activation strain is predicted from the material properties of the binder and thickness of the binder between particles. We note that there are different combinations of particles and binder for the activation process: aggregate with sand + cement and sand in cement, for example, offering the potential to optimize strength and mechanical properties.

In the case of ***compression*** the compressive stress-strain profile and strength (maximum stress) are shown to be a direct transformation of the tensile relationship in the inverse of Poisson's ratio. Rate effects for compressive strength are included by scaling the Poisson's Ratio with rate, where Poisson's Ratio tends to zero at high rates, such that tensile strains are not induced to generate damage. This approach predicts the general trend observed in the Hopkinson bar data as shown in Fig. 8.

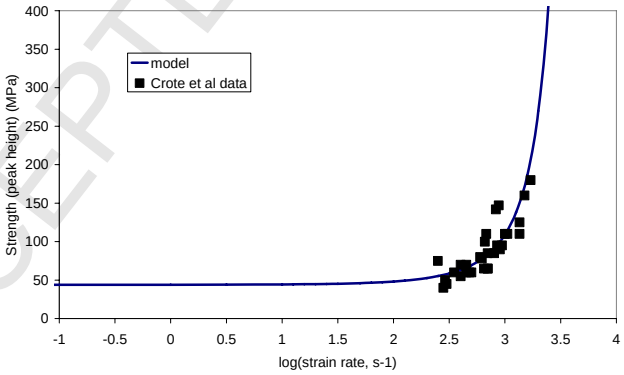

Fig. 8. Comparison of Porter-Gould constitutive model for concrete with high strain rate data [10]

Pressure hardening also comes directly from the description of damage. It is presumed that the material can only suffer damage when the strain state is tensile. The effect of pressure is to apply a

compressive strain onto the normal shape of the material and this compressive strain needs to be overcome in order that the tensile strain state for damage is achieved. In the first instance a very simple implementation of this physics is used. The compressive strain is taken to be the ratio of pressure, P, to bulk modulus, B, adjusted by Poisson's ratio, ν, and this is added to the activation strain.

$$\varepsilon_a \rightarrow \varepsilon_a + \nu \frac{P}{B} \tag{3}$$

The result of this variation of activation strain with pressure is to delay damage when under pressure – thereby allowing the material to achieve greater peak strength, figure 9. For already damaged material the effect will be to delay onset of further damage.

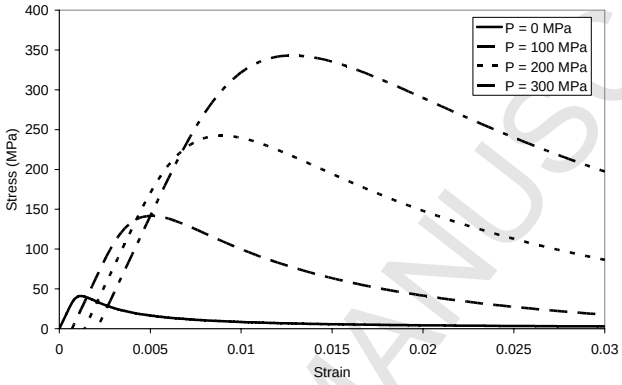

Fig. 9. Effect of modifying activation strain to account for pressure

This approach is entirely novel and is currently being implemented into the QinetiQ GRIM and customized DYNA hydrocodes. The model only has 4 constants, which are all measured or derived: bulk modulus, Poisson's ratio, an activation strain for the damage and a reference strain rate. An important potential future requirement is that this new generation of models will require additional experiments to measure certain aspects of the material response (e.g. dynamic Poisson's ratio) as opposed to a simple total stress.

4.1 Validation Of Model

The constitutive model is currently being implemented into the GRIM and DYNA hydrocodes and being tested by comparing a series of well defined stress-states in the mathematical package MathCAD with GRIM to ascertain whether the model is functioning correctly. This process has identified a number of issues concerning the implementation of the model as well as the method used to define various terms in the hydrocode as well as the interpretation of the experimental data to allow a direct comparison with the model with experimental data

The definition of Poisson's ratio at high strain rates, for example, is one such issue since this is fundamental to describing the high rate behaviour. The classical definition of Poisson's ratio is the ratio of the radial strain to the axial strain under quasi-static loading. At high strain rates the definition is less clear since there is a time delay due to wave propagation. For example in a plate impact experiment there is initially no lateral strain until release so the Poisson's ratio by definition is zero. Different

definitions of Poisson's ratio in the hydrocode lead to very different predictions for the stress state in the cell. Further theoretical development, coupled to carefully instrumented tests, is currently addressing this.

The other major issue is the change to a modulus-based model with damage, compared to a yield surface (i.e. plasticity). An interim approach is to define a pseudo yield surface to calculate the strain and stress increments, whilst preserving the physical basis of the model.

5. Conclusions

Within the UK a framework for a true physically based model for concrete has been defined and is considered a significant step forward in terms of both the EOS and a constitutive model having four parameters, which are either measured or derived. This has identified implications for model development within a hydrocode, principally the need for a modulus-based elasticity approach. It has also indicated the need for different measurements or analysis within the validation experiments. As part of an integrated framework consisting of precise experiments, simulations and material theory this is having a major effect in shortening the design and performance assessment cycles.

6. Acknowledgements

This work was funded and supported by various UK MoD Programmes.

References

[1] Church P, Goldthorpe B, Andrews T. A review of constitutive model development within DERA, *ASME PVP*, 199; **394**: 113-120.

[2] Porter D et al. Preparation development and preliminary application of novel equations of state for geological materials and ice, *1st Int. Conf. on Impact Cratering in Solar System*, ESTEC, 2006.

[3] Porter D. Interaction modelling of polymer properties, Marcel Dekker Inc, New York, 1995.

[4] Newman J. Deformation behaviour, failure mechanisms and design criteria for concretes under combinations of stress, *PhD Thesis*, Imperial College 1973.

[5] Bischoff P. H, Perry S. H. Compressive behaviour of concrete at high strain rates, *Materials and Structures* 1991; **24**: 425-450.

[6] Johnson and Holmquist; A computational model for brittle materials subjected to large strains, high strain rates and high pressures, *14th Int. Symp. Ballistics*, pp591-600, 1993.

[7] Armstrong R, Zerilli F, Dislocation mechanics based constitutive relations for material dynamics calculations', *Jnl. de Physique* 1988; **49**(C3): 529-535.

[8] Butler A, Goldthorpe B, Church P. A wide ranging constitutive model for bcc steels, *Jnl. de Physique* 1994; **C8**: 471-477.

[9] Goldthorpe B. A path dependent model for ductile fracture, *Jnl. Phys IV* 1997; **7**(C3): 705-710.

[10] Crote D L. et al. Dynamic behaviour of concrete at high strain rates and pressures. *Int. J. Impact Eng*., 2001; **25**: 869-886.